CFD simulation of compressed ethanol heating for cold start application in direct-injection engine

Hugo Marmori de Morais
School of Mechanical Engineering, University of Campinas

Arthur Vieira da Silva Oliveira
São Carlos School of Engineering, University of Sao Paulo

Rogério Gonçalves dos Santos
School of Mechanical Engineering, University of Campinas

ABSTRACT

Internal combustion engines that work with fuel at supercritical conditions can benefit from low viscosity, high mass diffusion coefficient, and low surface tension. These properties increase the fuel diffusion and its atomization. Also, heated fluid can improve the engine start and reduce pollutants emissions. However, to achieve these conditions, the fluid needs to be at a reduced temperature and a reduced pressure higher than 1, so it is necessary to heat the compressed fuel. This work concerns the heating of compressed ethanol and its behavior inside a cylindrical heating chamber with a cartridge heater placed concentrically with the chamber. We used the commercial software ANSYS Fluent to simulate the natural convection of ethanol at compressed and supercritical states. The heater works for a given time, about 4 seconds, promoting the increase in the fuel temperature, then it is turned off for 1 second to allow the thermal diffusion in the fluid. All the other walls are adiabatic. We evaluated the fluid behavior and temperature increase for two pressures higher than the critical. The change of thermodynamic properties affects the uniformity of the heated fluid across the heating chamber.

INTRODUCTION

The rising concern for the environment and the search for renewable energy sources require more eco-friendly solutions [1]. At this point, ethanol is a promising solution. Ethanol is a fuel that can be produced from biomass, or by agriculture where it consumes carbon dioxide for its production. The high diffusion of flex-fuel engines and the investments in internal combustion engines with ethanol has made the usage of this fuel a concrete reality and economically viable [2].

Ethanol also has higher octane levels, higher engine torque, and a lower emission rate of pollutants than gasoline [3]. However, it has a bad cold start performance, being necessary its pre-heating. This process increases the engine efficiency and lowers the pollutants emission [4]. Fluid heating studies are concentrated at low-pressure applications: Netto et al. (2022) modeled the nucleate boiling heat transfer for a gasoline surrogate at low pressures; Oliveira et al. (2017) studied gasoline and gasoline-ethanol blends nucleate boiling, also at low pressures. The lack of knowledge makes harder the fuel heating design aimed at direct injection engines.

Fluid is in the supercritical state when its temperature and pressure are higher than the critical temperature and pressure. In this situation, the fluid properties vary dramatically with the temperature, there is no visual differentiation of phases, and the fluid can behave like a liquid or a vapor [7]. They are used to cool down nuclear reactors and extract solvents. An internal combustion engine can benefit from supercritical fluid properties like low viscosity, high mass diffusion, and low surface tension. It can form a more homogenous mixture with air and optimize the power extraction from the engine [8].

This study presents the ethanol fuel at critical pressure inside a concentric cylinder geometry. We present the behavior of the streamlines and the temperature field at different times, focusing on the heat diffusion across the domain, so we can understand how the temperature rises and how commercial fuel heaters can heat compressed ethanol.

METHODOLOGY

Figure 1 shows the domain used in this study. It has two concentric cylinders and a path conducting the heater chamber to the pressure outlet that is used to maintain the pressure constant inside the domain representing a relief. The central diameter is 5 mm, the external diameter is 12 mm, and the path is 1 mm wide and 40 mm long We used the commercial software ANSYS Fluent to simulate the natural convection.

The central circle is at 276.9°C for 4 seconds to represent the heating process, while the other walls are adiabatic. After

this time, we turn off the heater, so the central circle becomes an adiabatic wall, and let the fluid settle for one second.

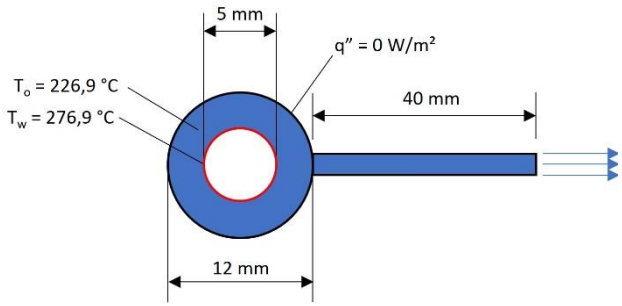

Figure 1 – Geometry of the heating chamber

This defined temperature at the heater does not represent an authentic fuel heater, in which the heat flux is defined. However, it allows us to have better control over the simulation, impeding the fluid from achieving temperatures not feasible for the equation of state used in this work. The initial temperature of the fluid is 226.9 °C. This condition is far from the ambient temperature, but it gives more consistent results than the simulations with ambient temperature, which had difficulties calculating the boundary layer. The temperature difference between the initial temperature and the wall temperature is 50 °C, an interval that passes through the critical temperature of 241.6 °C.

We simulated two pressures, 70 bar, and 80 bar. Both pressures are higher than the critical pressure of ethanol, 62.7 bar.

Figure 2 shows the ethanol properties – density, specific heat at constant pressure, dynamic viscosity, and thermal conductivity - for 70, and 80 bar pressure. The high variability requires an equation to calculate these properties. We used the real gas equation that is in ANSYS Fluent, these

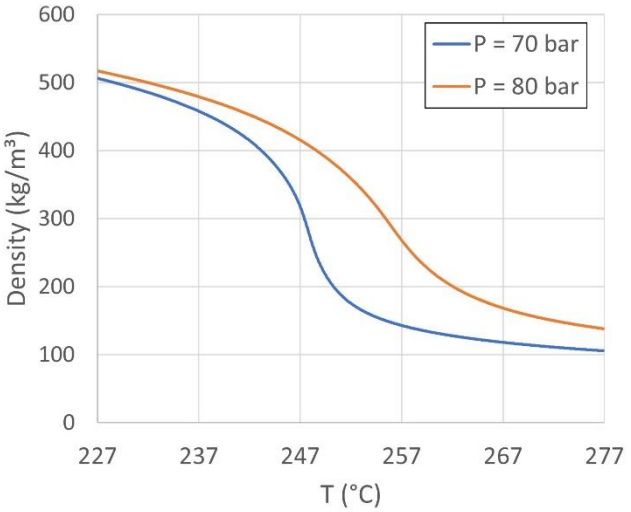

a)

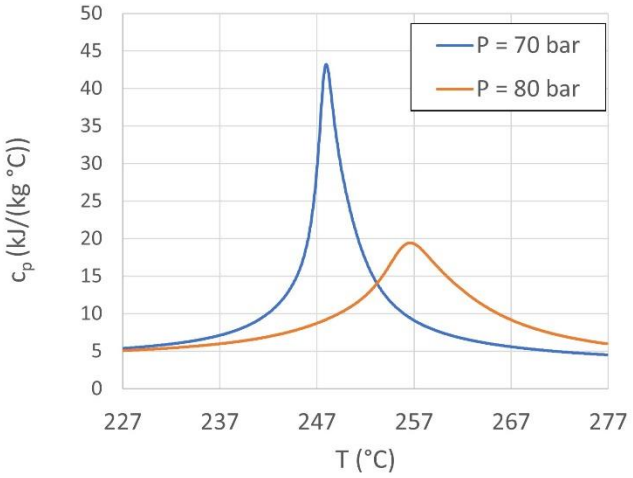

b)

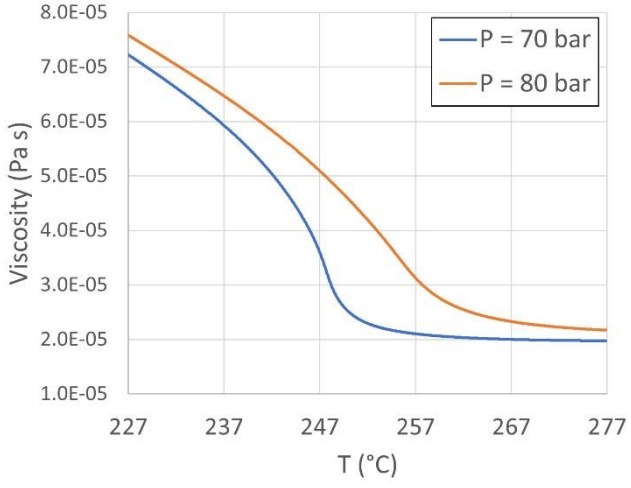

c)

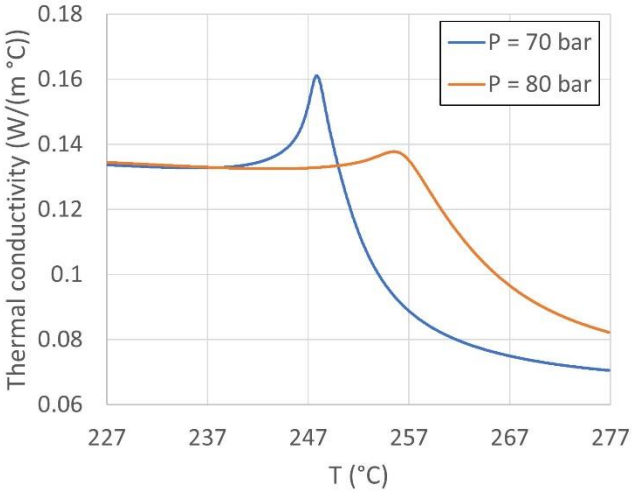

d)

Figure 2 – Fluid properties at 70 and 80 bar pressure, a) density, b) specific heat at constant pressure, c) dynamic viscosity, d) thermal conductivity

equations are from the NIST database. This way, we guarantee that a real fluid is in the model.

We did not use any turbulence model on Fluent. The calculated Rayleigh numbers with film temperature are 1.6×10^6 and 6.3×10^5. The most concerning Rayleigh number is 1.6×10^6 for the 70 bar pressure because, according to [9], at this point, there is the beginning of the formation of turbulent structures.

Figure 3 shows the mesh convergence test. The step time is 0.005 second, the same step that is used throughout the whole study. The variable used to evaluate is the maximum velocity at t = 0.3 second inside the domain. It is possible to visualize that beyond 80000 nodes there is no visible change in the maximum velocity. The chosen mesh has 82062 nodes

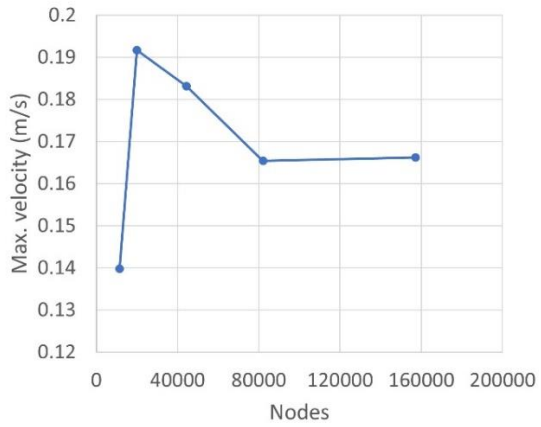

Figure 3 – Mesh convergence for the model presented

RESULTS

TEMPERATURE – Figure 4 shows the temperature field in the heating for 70 and 80 bar pressure, and times of 0.5, 2, 4, and 5 seconds. In the center of the domain, the fluid motion forms a higher temperature path, transferring heat from the heater to the fluid. The heated fluid hits the upper wall and disperses across the superior part of the geometry. For both pressures, this behavior occurs, but at 80 bar the temperature reached is higher than at 70 bar.

At 2 seconds, heated fluid fills the top of the domain. The convective path is barely visible due to the small temperature difference between it and the surrounding. Although there is heated fluid flowing to the relief path, the bottom of the domain is still at the initial temperature, so the heater is wasting energy. The symmetric behavior disappeared, mainly due to the high vorticity at the top and the pressure relief that moves the main path to the right. The 80 bar reached higher temperatures and the temperature distribution is more stratified than at 70 bar.

At 4 seconds, in figure 8, there is still fluid at the bottom at 226.9 °C. There is more heated fluid flowing out of the domain than at 2 seconds, which impedes the complete diffusion of temperature. The convective path is more inclined to the right than at 2 seconds flow time. The same trend from the previous flow time continues at 80 bar the fluid gets reaches a higher temperature than at 70 bar. Throughout the 4 seconds of flow time, the boundary layer deforms the temperature contour lines close to the wall the fluid motion prevents the wall temperature from reaching farther distances.

At 5 seconds, there is no visible movement of the fluid, so the major heat transfer process is the conduction, which is so slow that the bottom does not change temperature.

STREAMLINES – Figure 5 shows the streamlines in the heating for 70 and 80 bar pressure, and times of 0.5, 2, 4, and 5 seconds. The color scheme in the figure represents the velocity magnitude at that point.

At 0.5 seconds, the flow forms the main convective structure, the fluid gets warmer at the heater, accelerates, and goes up through the middle of the domain, then it hits the upper wall, and the return way is between two vortices formed at the top. There are 6 vortices formed at the top, 3 at each side. The middle vortex is bigger at 80 bar than at 70 bar. The streamlines that go from the top to the bottom of the chamber are similar. At 70 bar the maximum velocity is higher than at 80 bar due to the higher density variation, which happens at a smaller temperature for 70 bar.

At 2 seconds, there is a sinuous behavior of the streamlines. The vortices interfere with the convection path, the 3 distinguishable vortices from each side disappear, and only 2 remain at the top, the ones that are formed by the fast thin convective structure. The flow creates vortices in different regions of the domain. At 70 bar, the convective structure does not get a velocity of 0.12 m/s at the structure center, however, at 80 bar it gets, but at a smaller width.

At 4 seconds, the flow is more inclined to the right still an effect of the relief. There is also a higher velocity at the relief path than previously.

At 5 seconds, the streamlines do not show any path related to the strong natural convection that had been seen in the other flow times. Even the clear way out of the heating chamber through the relief is not as strong as it was. But there are still some low velocities on the upper left and on the right of the heater. This confirms that the conduction is the main way of heat transfer after the heater is turned off.

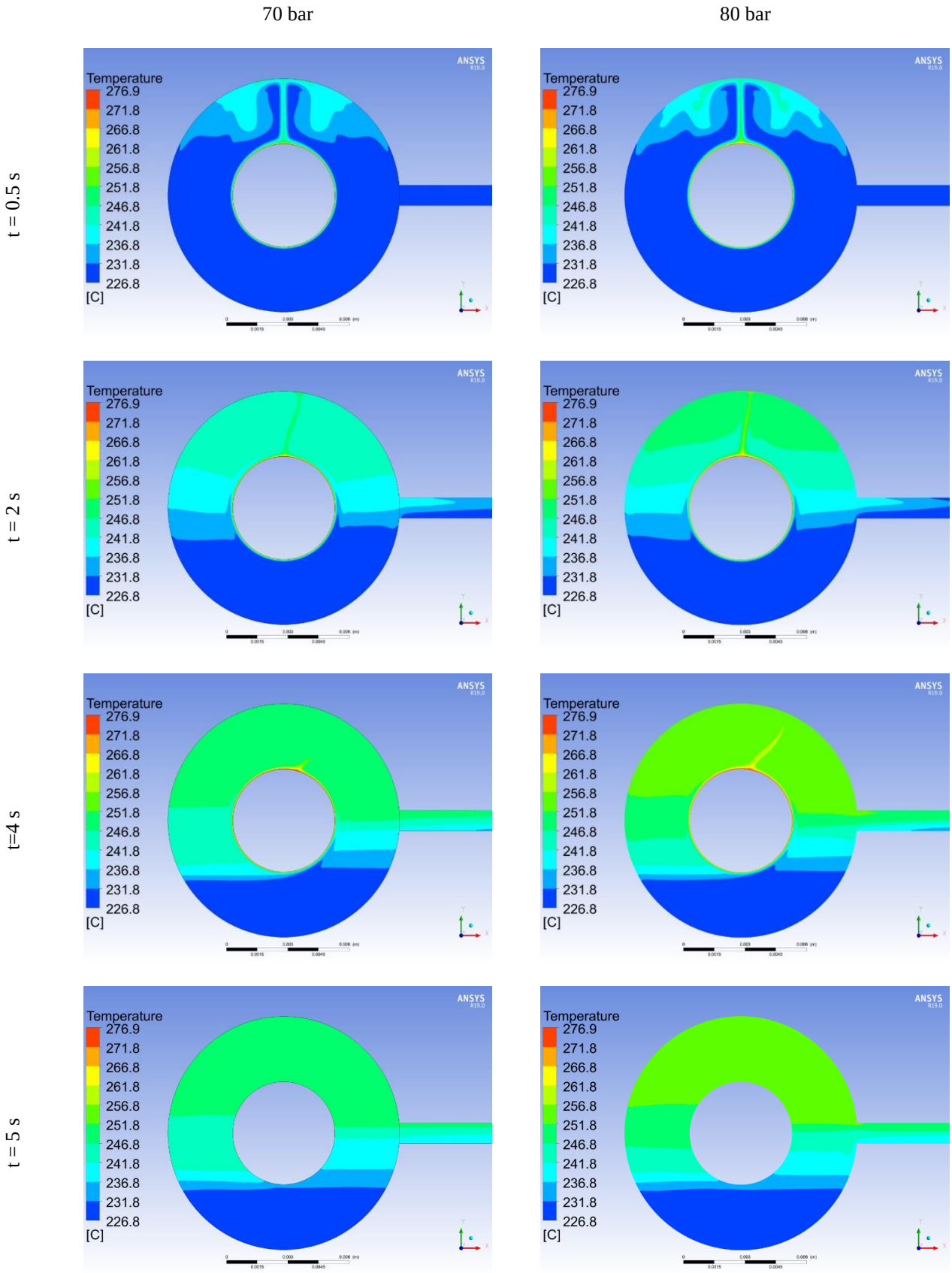

Figure 4 – Temperature field at t = 0.5, t = 2, t = 4, t = 5 for 70 bar and 80 bar

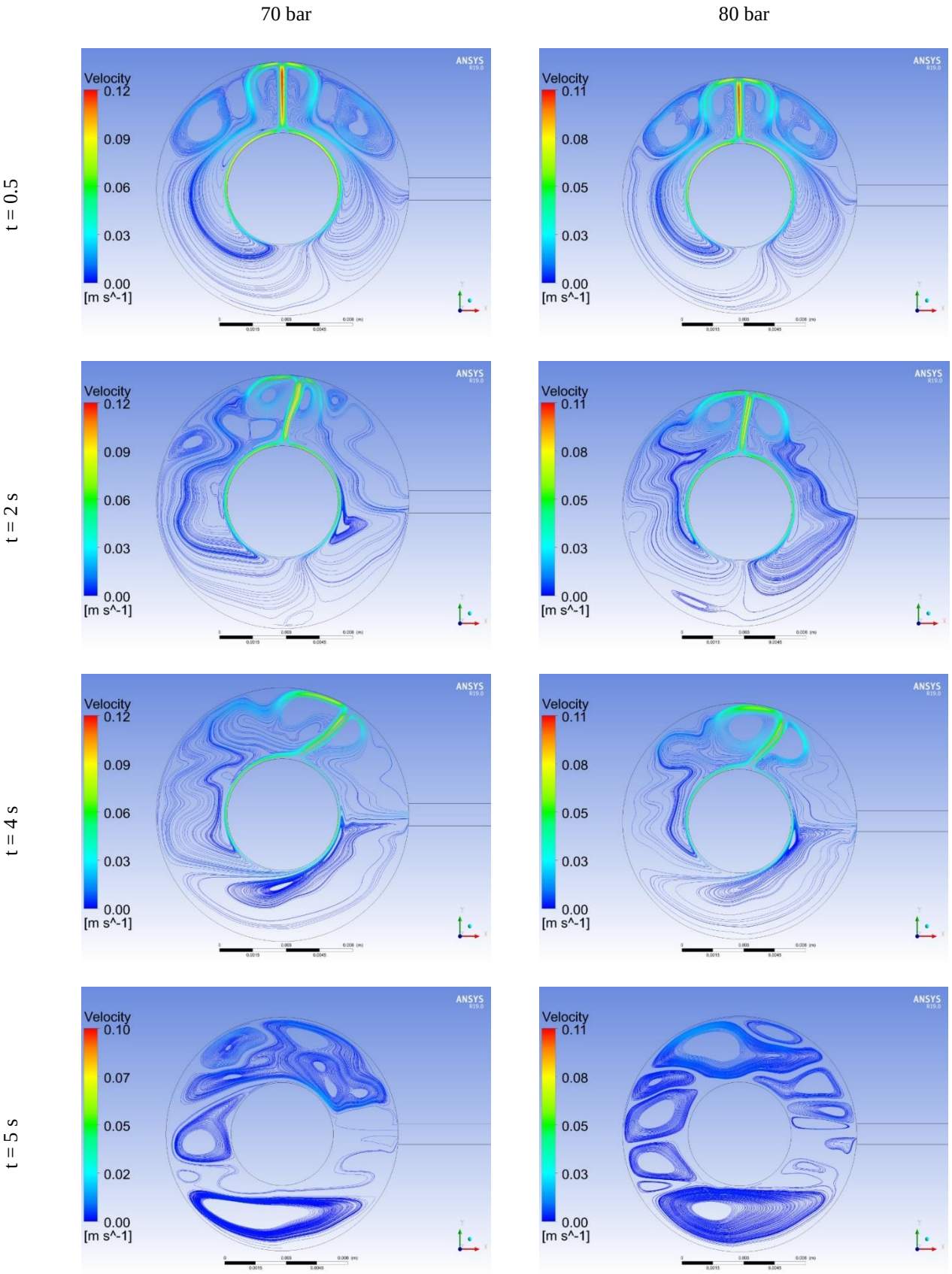

Figure 5 – Streamlines at t = 0.5, t = 2, t = 4, t = 5 for 70 bar and 80 bar

ANALYSIS – Figure 6 shows the total mass inside the chamber through the simulation. The mass of both pressures falls similarly, this happens due to the expansion of the fluid, and to keep the pressure at the same level, it is necessary that some fluid goes out of the domain by the relief. Although at 80 bar there is more fluid because the density is higher, it is at 70 bar that more fluid leaves the domain. After the heater is turned off, some fluid returns to the domain, but it is such a small amount compared to the amount that left the chamber, and in less than a second the increase stops.

Figure 7 contains the graph for the averaged behavior of the heat flux at the hot wall. The averaged heat flux is almost the same between the two pressures, so it can be said that in both simulations, ethanol received the same amount of energy. The heat flux gets smaller as time passes by because the gradient of temperature gets smaller, at 2 seconds, half of the chamber is not anymore at 226.9 °C.

Figure 8 shows the increase in temperature across the simulation. The fluid at 80 bar achieves a higher temperature than at 70 bar. This happened due to the specific heat, the higher it is, the more energy is required to increase the temperature. At 70 bar, the peak occurs at 248°C with a specific heat of 43 kJ/(kg °C) while at 80 bar the peak is at 256 °C and is only 19 kJ/(kg °C). So it is easier for the fluid at 80 bar to vary its temperature. Another effect is the decrease in temperature growth. This is associated with the smaller heat flux, and the fluid heated that leaves the chamber while there is a high amount of fluid in the initial temperature at the bottom.

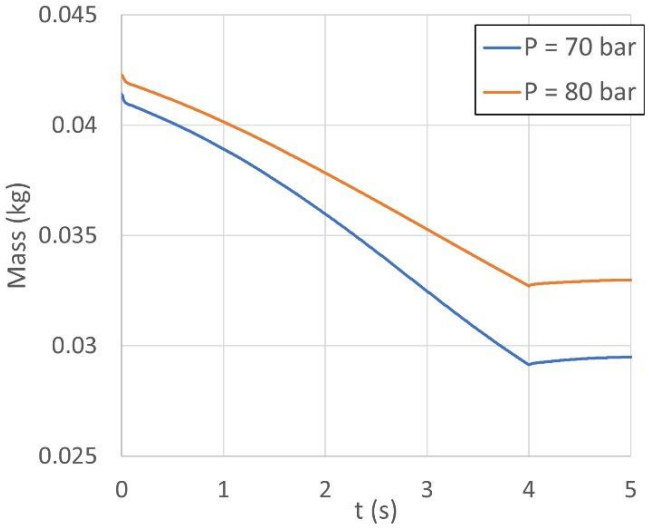

Figure 6 Mass balance inside the heating chamber for 5 seconds

CONCLUSION

In this study, we simulated the natural convection of compressed liquid ethanol at a temperature range between 226.9 and 276.9 °C inside a concentric cylinder using Equations of state for the real fluid at 70 bar pressure and at 80 bar pressure. In less than a second, the main convection structure is established. It takes hotter fluid from the heater to the top of the domain. As the simulation evolves, the behavior of the fluid becomes more chaotic, the convective path bends and the relief starts to play an important role in inclining the flow to the right

The fluid at 80 bar achieved higher average temperatures, and higher temperatures at the top of the domain, while at 70 bar the maximum velocity was higher.

The fluid received heat at an almost identical rate, but this similarity did not reflect in mass and temperature. At 70 bar the fluid was more subjected to mass variations, and at 80 bar the temperature increase was bigger.

The variable properties of a compressed liquid that achieves the supercritical points in some regions affect the flow of the fluid due to the natural convection and are linked to the temperature and mass variations. The heat flux might be the same for different levels of pressure at a supercritical state, but this point needs deeper research.

NEXT STEPS – This is the beginning of a more complex study to understand the behavior and the benefit of heating a supercritical fluid for fuel heating applications. The models can and will be improved for the next simulations. The first step is to use a turbulence model, the high number of vortices formed and the proximity to the experimental transition might be affecting the simulation. The second step is to use a three-dimensional domain closer to commercial heater present in the market. And a third step is to implement initial and boundary conditions closer to the application, like a fixed heat flux and a initial temperature equal to the ambient temperature.

ACKNOWLEDGMENT

The authors acknowledge the financial support received from the program Rota 2030 in form of a scholarship.

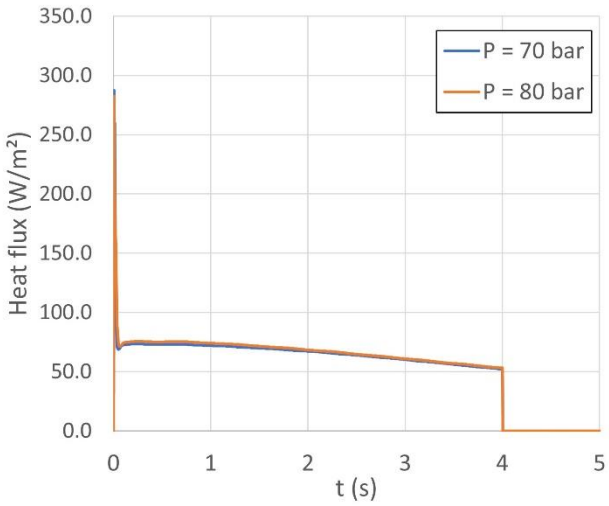

Figure 7 - Averaged heat flux at the heated wall for 5 seconds

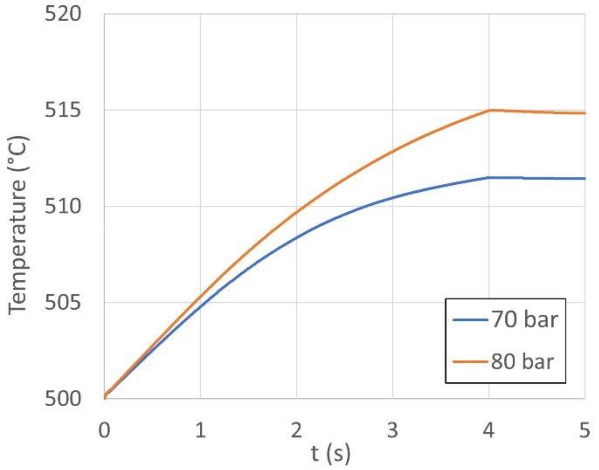

Figure 8 - Mass-averaged temperature at the heating chamber for 5 seconds

REFERENCES

[1] Wang, Y., and Zhensheng, L. "Numerical Study on Fuel Preheating at Cold Start Phase in an Ethanol Flex Fuel Engine." Journal of Energy Resources Technology, v. 140.8 (2018).

[2] Marques, D. O., et al. Combustion assessment of an ethanol/gasoline flex-fuel engine. Journal of the Brazilian Society of Mechanical Sciences and Engineering, v. 39.4 (2017): 1079-1086.

[3] Nakata, K., et al. The effect of ethanol fuel on a spark ignition engine. No. 2006-01-3380. SAE Technical Paper, 2006.

[4] Huang, Y., and Guang, H. "Investigation of the effect of heated ethanol fuel on combustion and emissions of an ethanol direct injection plus gasoline port injection (EDI+ GPI) engine." Energy Conversion and Management 123 (2016): 338-347.

[5] Netto, A. T. S., Oliveira, A. V. S., and Santos, R. G. "Discrete model to estimate nucleate boiling heat transfer coefficient with gasoline using a double-log-normal distribution function." Journal of the Brazilian Society of Mechanical Sciences and Engineering 44.1 (2022): 1-16.

[6] Oliveira, A. V., Alegre, G. H. M., and Santos, R. G. "A comprehensive experimental study on nucleate boiling in gasoline and gasoline-ethanol blends." Experimental Thermal and Fluid Science 88 (2017): 134-144.

[7] Pioro, I. L. "Supercritical-Fluids Thermophysical Properties and Heat Transfer in Power-Engineering Applications." Advanced Supercritical Fluids Technologies. IntechOpen, 2020.

[8] Song, Yukun, et al. "Numerical investigation of the combustion characteristics of an internal combustion engine with subcritical and supercritical fuel." Applied Sciences 10.3 (2020): 862.

[9] Kuehn, T. H., and Goldstein, R. J. "An experimental study of natural convection heat transfer in concentric and eccentric horizontal cylindrical annuli." (1978): 635-640.